Microstructural and Mold Resistant Properties of Environment-Friendly Oil-Modified Polyurethane Based Wood-Finish Products Containing Polymerized Whey Proteins

Nareen C. Wright, Jiancai Li, Mingruo Guo

Department of Nutrition and Food Sciences, University of Vermont, Burlington, Vermont 05405

Received 31 March 2005; accepted 15 June 2005
DOI 10.1002/app.22432
Published online in Wiley InterScience (www.interscience.wiley.com).

ABSTRACT: Environmental concerns associated with the level of volatile organic compounds used in surface coatings have stimulated increased scientific research toward novel methods of developing environment-friendly coatings. Prototype wood finish products containing polymerized whey proteins (PWP) were formulated. The microstructural characteristics of dry films prepared from environment-friendly wood finishes containing PWP were examined using atomic force microscopy (AFM) and confocal laser scanning microscopy (CLSM). The susceptibility of the coatings to microbial degradation was also examined using an accelerated mold test. AFM analysis revealed that increased addition of PWP resulted in films with increased surface roughness, decreased number of voids, and increased void size due to excessive aggregation among polymer components. CLSM analysis showed that the PWP distribution in the films is enhanced by homogenization of the coating mixes. There was no significant increase ($P > 0.05$) in mold growth between panels coated with finish containing PWP and those without PWP. Test panels coated with formulation containing PWP and low levels of biocide (0.3%) resulted in a significant decrease in mold growth in comparison to commercially available water-based polyurethane coatings ($P < 0.05$). © 2006 Wiley Periodicals, Inc. J Appl Polym Sci 100: 3519–3530, 2006

Key words: wood finish; whey proteins; polyurethanes; microstructure; mold resistance

INTRODUCTION

The film forming process of polymer materials used in paint and surface coatings such as wood finish serves as an integral parameter when assessing the functionality and performance of the coatings. Molecular interactions among polymer components have a considerable impact on the final products' performance. To improve the film quality and structure of surface coating materials, a clearer understanding of the film formation mechanism is necessary. Early studies on microstructure analysis demonstrated that particle size, orientation, and structural cohesiveness can improve functional properties of surface coatings.[1] Over the years, a wide range of microstructure imaging techniques, including transmission electron microscopy (TEM), scanning electron microscopy (SEM), confocal laser scanning microscopy (CLSM), and atomic force microscopy (AFM), have been used to analyze the microstructure of surface coatings.[2–5]

AFM is a topographical tool used to illustrate the surface morphology of a sample with limited preparation steps. The versatility of AFM is reflected in its many modes of operation and its capability of producing surface images at ambient conditions in air or in fluids.[6] AFM uses an atomically sharp tip to map out the contour of a sample's surface, with subnanometer resolution and is capable of reconstructing these images to produce a three-dimensional topography of the sample.[7] The probe tip which is connected to a flexible cantilever scans the surface of the sample in the x–y plane, and perturbations caused by physical changes within the structure deflect the cantilever in the z-direction. By imaging the sample in its native state and providing an array of information, such as frictional property measurements, detection of phase differences, and mechanical properties relating to force measurements, AFM has proven to be a good imaging tool for analyzing surface structure detail. In the area of surface coating, AFM has been used in contact and tapping mode to perform hardness measurement, evaluate adhesion and thin film integrity, detect material property differences on heterogeneous surfaces, and to describe the extent of particle coalescence during film formation.[3,8,9]

Correspondence to: M. Guo (mguo@uvm.edu).
Contract grant sponsor: USDA CSREES.

Another useful imaging technique capable of providing unique insight on the film structure of surface coatings is CLSM. The power of CLSM lies in its ability to effectively distinguish fluorescently stained components within a sample. Digital images of a sample, in CLSM, are obtained as a result of optical sectioning produced by scanning a laser beam across a specified area of the sample. Unwanted fluorescence from within the sample is filtered out by spatial filters to produce images from only the focal plane of interest.[9] The uniqueness of CLSM allows for the exact position of a molecule to be identified.[10] One of the major challenges in CLSM is photobleaching of the fluorochromes such that stained areas of interest are no longer visible. A recent study in the area of surface coatings using CLSM is to detect structural changes in clear lacquers due to the addition of silica matting agents.[4]

Microbes are ubiquitous and can be detrimental to the functionality of surface coatings. Infestation by microorganisms can facilitate changes in the film structure, impairing its mechanical and protective properties. There are many microbial species (bacteria, fungi, and algae) responsible for biodegradation of water-based coatings.[11] Water activity, pH, temperature, and available nutrients are some of the key parameters that can affect the proliferation of microorganisms in surface coatings. Growth conditions required for the three major types of microorganisms in surface coatings was published by Dunk.[11] Among the three types of microorganisms, fungi are more prone to cause microbial degradation of interior surface coatings due to high humid conditions. Fungi are capable of growing well at room temperature, under acidic conditions, requiring relatively low water activity and oxygen. Once the growth has sporulated, disfigurement and discoloration of the coated surface becomes very apparent. The esthetic appeal of the product is lost and degradation of the substrate is inevitable.

The addition of biocides is commonly used to alleviate the growth of microbes within surface coatings. There are many different biocides specific to particular microorganisms, depending on the state of the coatings (solution vs. dry film).[12] With the coating industry moving toward producing more environment-friendly products, the safety of biocides with respect to health and environmental concerns is also taken into consideration before incorporating as an additive into a product.

It has been extensively studied and documented that whey proteins can be polymerized through heat treatment to form surface coating films.[13,14] Whey, a by-product of cheese making, is produced in abundance each year and is disposed of as a waste material when not fully utilized.[15] Therefore, considerable efforts are being made to find new uses for whey to alleviate concerns of whey disposal. The incorporation of whey proteins in formulating environment-friendly wood finishes provides a promising alternative for further utilization of whey.[16,17]

The objectives of this study were to analyze the structural characteristics of prototype environment-friendly water-based wood finish coatings containing polymerized whey proteins, using different imaging techniques and to investigate the susceptibility of the coatings to microbial growth using an accelerated mold resistance test.

EXPERIMENTAL

Materials

Whey protein isolate (WPI, ALACEN® 895, 93.5% protein) was gifted from NZMP (North America) Inc. (Santa Rosa, CA). An oil-modified polyurethane dispersion (PUD, Spensol F97-MPW-33) was obtained from Reichhold Inc. (Morris, IL). Amicure™ TEDA Crystalline catalyst (Air Products Inc., Allentown, PA), BYK-345 surfactant (BYK-Chemie USA Inc., Wallingford, CT), Acrysol™ RM-2020 NPR rheology modifier (Rohm and Haas Company, Bridgeport, NJ), Drewplus L-405 defoamer (Drew Industrial of Ashland Canada Corp., Ajax, Ontario, Canada), and Proxel® GXL preservative (Avecia Inc., Wilmington, DE) were used to formulate the prototype wood finish coating formulations. Alexa Fluor® 647 carboxylic acid, succinimidyl ester (Molecular Probes Inc., Eugene, OR) was used for staining the whey proteins in the film samples. Dimethylsulfoxide (DMSO, Sigma Chemical Co., St. Louis, MO) was used as a solvent for the protein dye. Phosphate Buffered Saline (PBS, 0.01*M*) with 0.15*M* NaCl was used to wash away unincorporated dye. Mold strains used to inoculate the chamber were *Aureobasidium pullulans* (ATCC 9348), *Aspergillus niger* (ATCC 6275), and *Penicillium Sp*. 12667 (American Type Culture Collection, Manassas, VA). BUSAN® 1292 (Buckman Laboratories, Inc., Memphis, TN) was used as a biocide.

Wood finish coating formulations

Thermally polymerized at 90°C for 30 min, WPI solution (10% protein) was used as a cobinding material in formulating the water-based environment-friendly wood finish products. Prototype coating formulations were prepared by mixing different levels of polymerized whey proteins (PWP) solution, PUD, water, and other additive components. The levels of each variable component for the different formulations are listed in Table I. For AFM analysis, dry films from coating formulations containing 10.5–31.5% of PWP were examined. For further illustration of the protein distribution by CLSM, an additional formulation containing 48% PWP was developed. Surface films from the coat-

TABLE I
Levels of Three Major Ingredients in Prototype Coating Formulations

	Coating formulations			
Ingredient	F1	F2	F3	F4
PUD[a] (%)	60.45	57.27	54.09	33.93
PWP[b] (%)	10.50	21.00	31.50	48.00
Water (%)	24.85	14.92	4.97	4.50

[a] PUD, Oil-modified polyurethane dispersion resin.
[b] PWP, Polymerized whey protein solution.

ing formulations based on only each of the two binder components, PUD or PWP, were also analyzed as controls for further comparison.

Atomic force microscopy

AFM was employed to examine the topographical surface contour of the dry film after 48 h of conditioning in an environmental chamber (ENVIRONAIR System, model 11–13RL, East Longmeadow, MA) at 23 ± 2°C and (55 ± 5)% RH. The samples were fixed to a glass slide using double-sided tape and securely fastened to the microscope stage for viewing. The samples were imaged in contact mode in air with a Digital Instruments BioScope (Digital Instruments, Santa Barbara, CA) positioned on an Olympus IX 70 inverted light microscope (Olympus America, Inc., Melville, NY). The entire imaging system was placed on a MICRO-g vibration isolation system (Technical Manufacturing Corp., Peabody, MA) to minimize vibrational disturbance. Captured images were obtained using a cantilever with electron beam deposited (EBD) tips fabricated on 200-μm thin-legged oxide sharpened pyramidal tipped (nominal radius 20 nm) silicon nitride probes (spring constant 0.38 N/m.s). Off-line Nanoscope IIIa (version 4.23rb© 1998) section analysis software was used to conduct zero order flatten, surface roughness measurements, and to erase scan line. Images were obtained at 30, 5, and 2.5-μm scan size and at a scan rate of 1 Hz.

Confocal laser scanning microscopy

CLSM was used to determine the protein distribution within the dry film coatings. A series of Alexa Fluor® 647 dye concentrations (50, 25, 10, 5, 1, and 0.5 μg/mL) were prepared using PBS as a diluent to determine the necessary stain concentration needed for labeling the proteins in the dry films. A concentration of 10 μg/mL Alexa Fluor® 647 solution was identified to be the optimal dye concentration for CLSM analysis of the samples.

Small pieces of each sample, ~0.5 cm × 1.0 cm, were stained by immersing the sample for 15 min in the dye solution, after which the stained samples were rinsed in PBS solution for an additional 15 min (three 5-min intervals). Images were obtained using a BioRad MRC 1024 Confocal Scanning Laser (Hercules, CA) mounted on an Olympus BX50 upright microscope. The absorbance and fluorescence emission maxima for Alexa Fluor succinimidyl ester are 650 and 665 nm, respectively. The filter for 647 excitation emission was 680df32 and 522df32 for 488 excitation emission. Sample images obtained illustrate autofluorescence as a green color and protein fluorescence as blue. Confocal micrographs were obtained at both 20× and at 60× oil-immersion objectives using a 2.5 electronic zoom. The same settings were used to compare all samples for illustrating the difference in fluorophore concentration as PWP content increased. Protein distribution was also illustrated based on optimizing the dynamic range of the gray scale intensity, using an overlay which discriminated between the highest and lowest pixel intensity. Multiple images were obtained for one sample from different sections of the film to ensure a true representation of its microstructure.

Mold resistance test

A modified D3273–94 method of American Society for Testing and Materials (ASTM) was used to test the resistance of the newly developed coatings to mold growth. The tank chamber was made from high density polyethylene (HDPE) material having dimensions of 17.75 in. × 26.75 in. × 18 in. The conditions in the chamber were maintained at 33 ± 1°C and 95–98% RH. The mold testing chamber was placed in an environmental chamber (23 ± 2°C, 55 ± 5% RH). An internal humid environment within the mold tank was created by placing water at the bottom of the tank (about 10 in. deep). Two Proquatics Thermofilters (Pacific Coast Distribution, Inc., Phoenix, AZ) placed on opposite sides of the tank were used to uniformly heat the water at the bottom of the tank. Greenhouse potting soil (25% peat moss, pH 5.5–7.6) was uniformly distributed on the bottom of a stainless steel tray (16.75 in. × 24 in. × 16.5 in., 150-metal mesh), raised ~6 in. above the water surface. A pictorial illustration of the mold resistance testing tank chamber is shown in Figure 1.

The system was allowed to equilibrate for 24 h before inoculating with mold spores. Mold suspensions of three cultures (*A. pullulans*, ATCC 9348, *A. niger*, ATCC 6275, and *Penicillium Sp*. 12667) were distributed evenly over the surface of the soil. Sporulation and equilibration of the molds were allowed for 2 weeks before conducting a viability test. Potato dextrose agar (PDA) plates were left open and face-up in the mold tank for 1 h before incubating at 33 ± 1°C for 3 days to check the viability status of the molds. After sufficient mold growth (covering the complete surface of the plates) was observed on the PDA plates, the

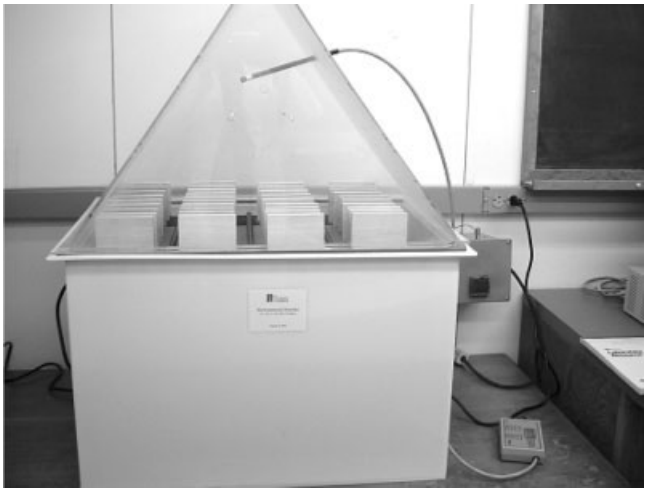

Figure 1 Mold resistance test tank chamber.

coated test panels (Ponderosa pine wood) were placed into the mold chamber for testing.

There were seven treatments administered to the test panels. The treatments of the panels were as follows: uncoated test panels served as a control, simple PUD (without PWP and biocide) coating, PUD plus 19% PWP (PUD–PWP) coating containing no biocide, simple PUD coating plus 0.3% biocide, PUD–PWP coating plus 0.3% biocide, commercial water-based polyurethane coating, and commercial water based acrylic–polyurethane coating. The coated test panels were conditioned in the environmental chamber for 4 days before placing into the mold testing chamber. All panels were randomly distributed and placed upright on horizontal bars within the tank. Panels used in this study were replicated in triplicate.

Visual rating of the test panels was conducted once a week for 6 weeks based on the level of mold growth using a photographic rate scale of 0–10 (ASTM D 3274–95), in which a rating of 10 represents no growth and 0 represents complete surface coverage. Digital and microstructure images were obtained once a week using a Digital Still Camera FDMavica (Sony Corp., Japan) and an Intel® Play™ QX3 Computer Microscope (Molecular Expressions, Tallahassee, FL).

Statistical analysis

Repeated measures analysis of variance was conducted on mold test data using SAS (SAS Institute Inc., Cary, NC). Significant differences in mold growth were reported at P-values < 0.05.

RESULTS AND DISCUSSION

Incorporation of polymerized whey proteins into a waterborne resin based coating mix has been shown to produce environment-friendly prototype wood finish coatings with low levels of volatile organic compounds.[16,17] The coating performance (e.g., mechanical and water resistant properties) of these newly de-

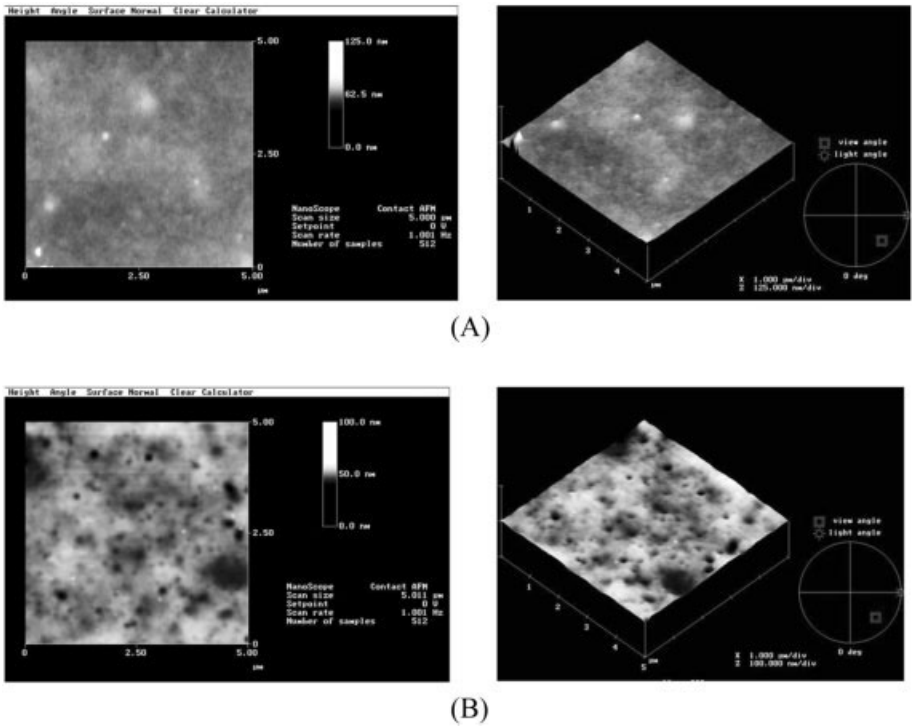

Figure 2 AFM micrographs of control coatings: (A) simple PWP; (B) simple PUD.

TABLE II
Atomic Force Microscopy (AFM) Surface Roughness Measurements of Prototype Coating Formulations and Commercial Products

Formulation	Surface roughness values (nm)
Simple PWP[a]	1.529
Simple PUD[b]	2.096
PUD–PWP[c] (10.5% PWP)	2.594
PUD–PWP[c] (21.0% PWP)	5.138
PUD–PWP[c] (31.5% PWP)	5.203
C1[d]	5.967
C2[e]	3.515

[a] Simple polymerized whey protein coating.
[b] Simple oil-modified polyurethane resin coating.
[c] Blended oil-modified polyurethane and polymerized whey protein coatings.
[d] C1, Commercial water-based polyurethane coating.
[e] C2, Commercial water-based acrylic–polyurethane coating.

veloped coatings were comparable to those of commercial counterparts.

AFM analysis

AFM micrographs of dry films based only on PUD binder or simple PWP binder are shown in Figure 2. The images reveal that both binders form a relatively smooth polymer matrix with low surface roughness values (Table II). PUD films portrayed voids within its structure which were not visible in PWP micrographs. The surface porosity was probably due to dissolved gases escaping from the film during casting and drying.[18]

The effect of mixing the two polymers is shown in Figure 3. Addition of PWP at 10.5% produced surface images with increased voids and higher surface roughness values compared to both simple PUD and simple PWP films. As PWP content further increased to 21%, fewer voids were apparent and an increase in pore size occurred especially for films at 31.5% PWP incorporation. Surface roughness measurements revealed that micrographs obtained from simple PWP films had surface roughness values of 1.529 nm and films containing 31.5% PWP resulted in the highest surface roughness measurement, 5.203 nm. AFM has been used to determine the best ratio for producing the most extensive particle coalescence within the blended surface coating of soft and hard polymer mixtures.[3,11,19] Ming and Meier showed that in addition to polymer blend, the drying conditions of the surface coating can also have a considerable impact on the polymer surface structure.[19] In their study, the number of voids and surface roughness measurements decreased with increasing curing temperature to form a tight-knit polymer structure. The surface roughness measurements also decreased exponentially with curing time. Increased compatibility of the two polymers correlated with decreased surface roughness values, producing a smooth film without

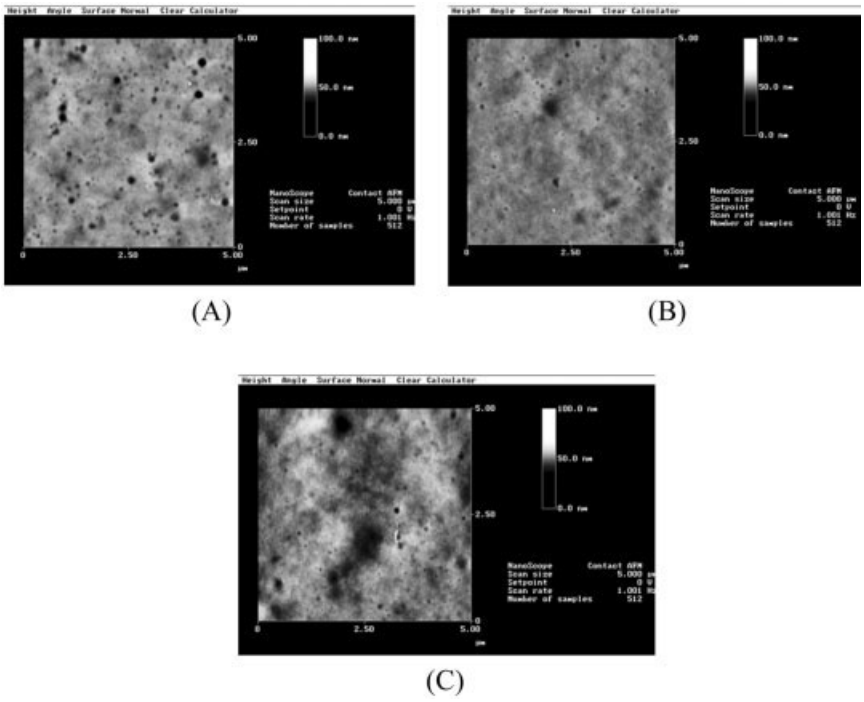

Figure 3 AFM micrographs of PUD–PWP composite coatings: (A) with 10.5% PWP; (B) with 21.0% PWP; (C) with 31.5% PWP.

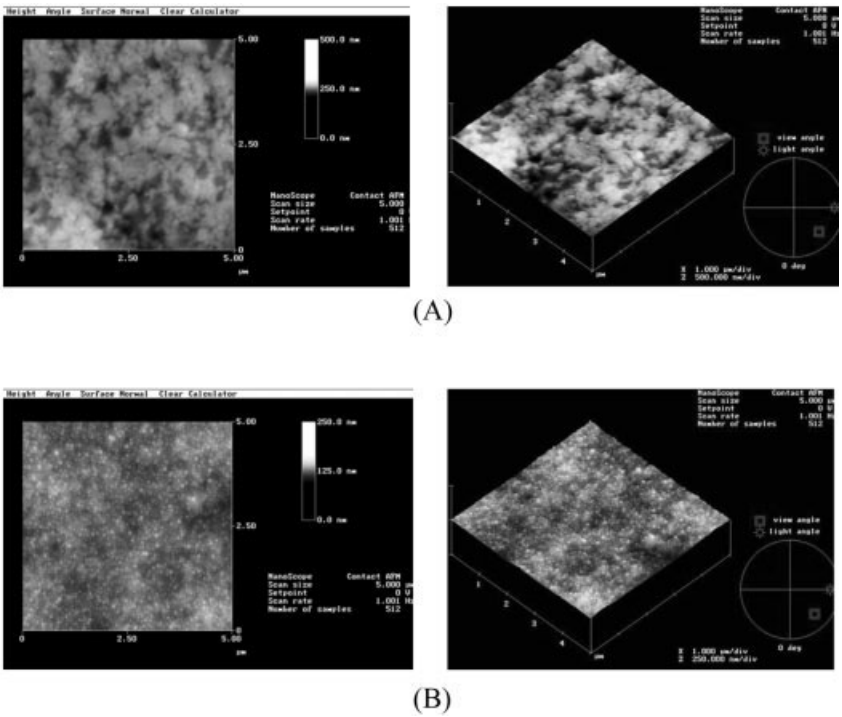

Figure 4 AFM micrographs of commercial water-based coatings: (A) simple polyurethane; (B) hybrid acrylic–polyurethane.

voids. Because of the high resolution of AFM, voids/depressions/pits are commonly observed within the film structure of surface coatings when excessive coalescence of the particles is not achieved.[20] AFM surface analysis conducted on coatings and paints has often used surface roughness measurement as a means of obtaining quantitative data on the surface structure.[21,22] These studies have often associated surface roughness measurement with the extent of particle coalescence within the film. Increased particle coalescence tends to produce smoother films correlating with increased film strength.

Micrographs of two commercial coatings examined by AFM are shown in Figure 4. The surface structure depicts large clumps of features protruding from the surface with voids/depressions throughout the polymer matrix of simple water-based commercial polyurethane film [Fig. 4(A)]. Figure 4(B) represents a hybrid commercial coating of acrylic–polyurethane polymers. Individual particles, with limited coalescence, were seen packed within the film structure having dimensions of less than 150 nm in diameter and 8 nm in height. Based on *z*-range measurements of the surface structure for both commercial coatings, the acryl-

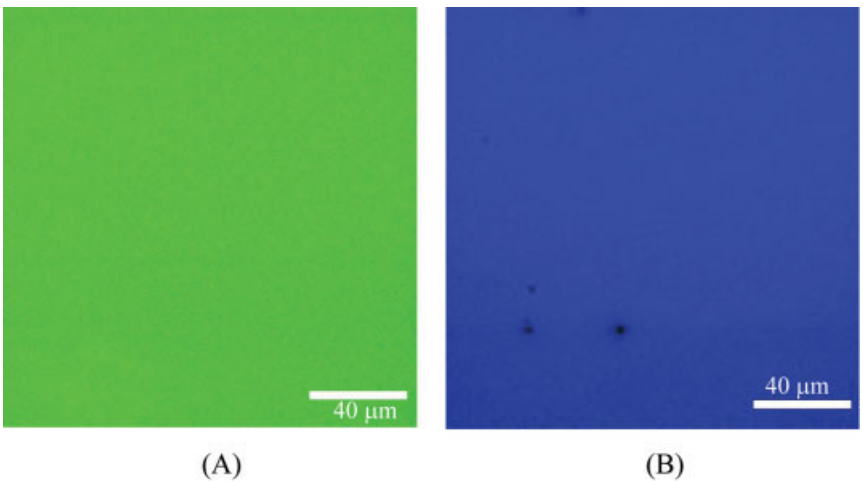

Figure 5 CLSM images of control coatings: (A) simple PUD; (B) simple PWP. [Color figure can be viewed in the online issue, which is available at www.interscience.wiley.com.]

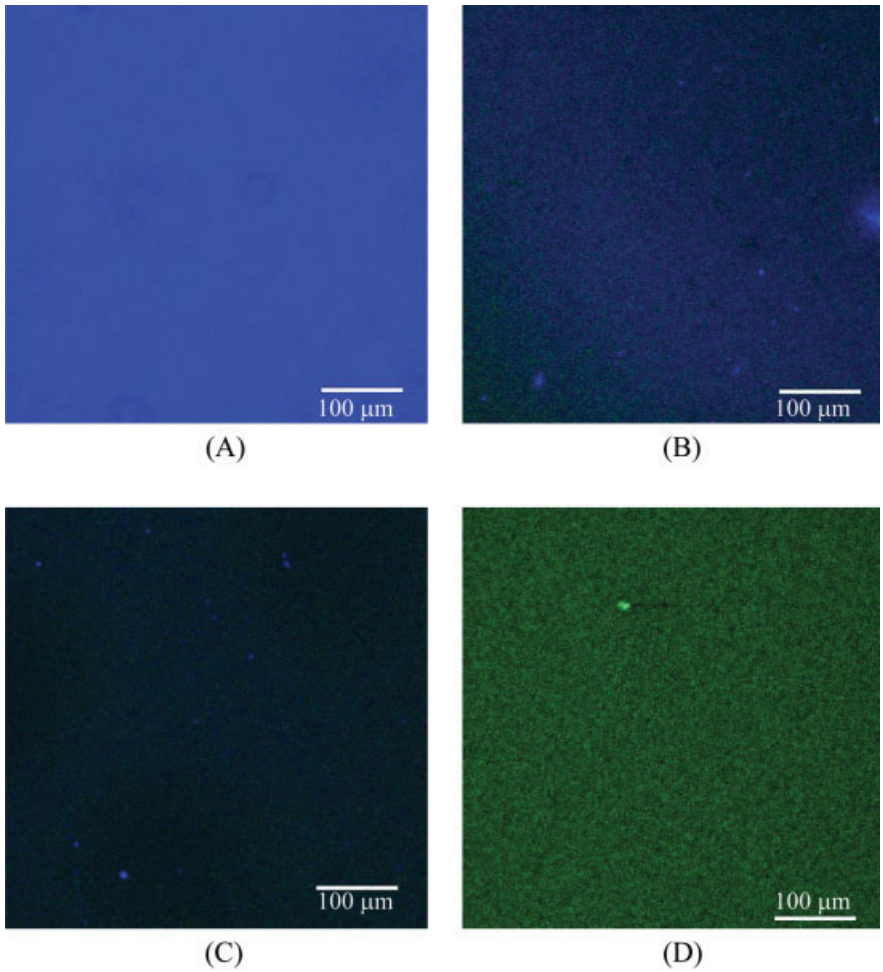

Figure 6 CLSM images of PUD–PWP composite coatings: (A) with 48.0% PWP; (B) with 31.5% PWP; (C) with 21.0% PWP; (D) with 10.5% PWP. Scale bars represent 100 μm. [Color figure can be viewed in the online issue, which is available at www.interscience.wiley.com.]

ic–polyurethane hybrid coating had smaller particle size dimensions, which contributed to its flat surface measurement. It has become a common practice in the coating industry to blend different polymer materials to reduce cost and toxicity for improving the environmental and economic aspects of the coating products.[22]

CLSM analysis

CLSM micrographs of simple PUD and PWP films are shown in Figure 5. As expected, no fluorescence in the far-red (647 nm) channel was observed in simple PUD films [Fig. 5(A)]; only autofluorescence in the green channel, 488-nm excitation, was observed due to the polyurethane polymer material. Extensive fluores-

TABLE III
Confocal Laser Scanning Microscopy (CLSM) Settings for Illustrating Dye Concentration with Increasing Polymerized Whey Protein Content

Settings	Far red	Far green
Laser power	10%	10%
Iris	4	4
Gain	1452.4	1452.7
Offset	−4	−5.5

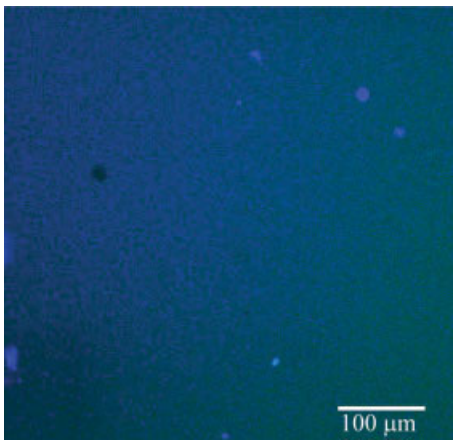

Figure 7 CLSM image shows distribution of protein within PUD–PWP composite coating containing 10.5% PWP at increased laser setting. [Color figure can be viewed in the online issue, which is available at www.interscience.wiley.com.]

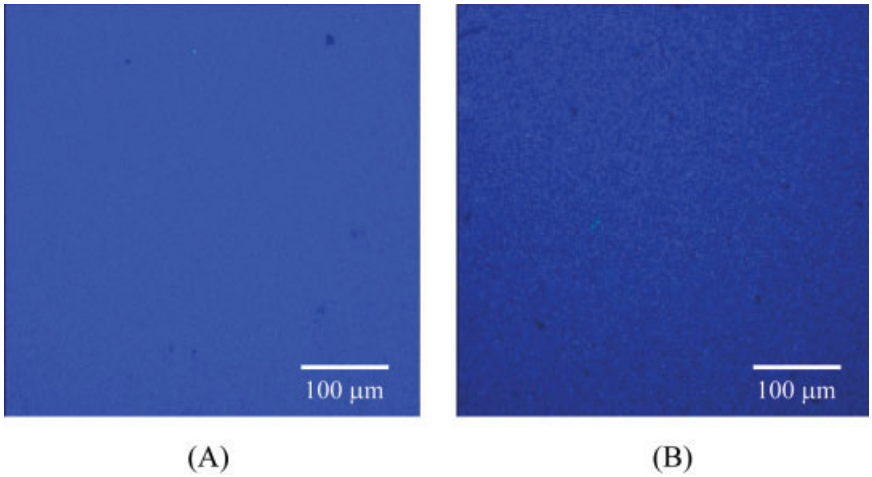

Figure 8 CLSM images of PUD–PWP composite coating containing 48.0% PWP at ×20 magnification: (A) top view; (B) bottom view. [Color figure can be viewed in the online issue, which is available at www.interscience.wiley.com.]

cence in the 647-nm dye channel was clearly illustrated in films containing only PWP binder material, with no visible autofluorescence [Fig. 5(B)]. Visible voids illustrated in simple PWP micrographs have been previously observed by CLSM imaging and were attributed to air pockets trapped within the film structure.[23] These micrographs demonstrated that Alexa Fluor 647 is an effective dye for distinguishing between PWP and PUD within the blended formulations.

Figure 6 illustrates the difference in dye concentration as the percentage of PWP increased. The images in Figure 6 were obtained at 8-μm optical depths, using a constant laser setting (see Table III) at 20× magnification. Figure 6(A) showed intense dye staining at high levels of protein content (48%) with large protein particulates visible. As PWP content decreased, dye staining became less apparent while protein aggregates remained visibly embedded within the polymer structure. At 10.5% PWP incorporation (Fig. 6(D)), no visible protein was observed within the matrix. However, when the laser settings were increased (30% laser power, iris 3.8, gain 1425, and offset −7) dye stain became more apparent, illustrating a faint distribution of PWP (Fig. 7). The Alexa Fluor® 647 stain consecutively appeared brightest in micrographs containing the highest level of PWP content regardless of the laser settings. The increase in dye stain intensity

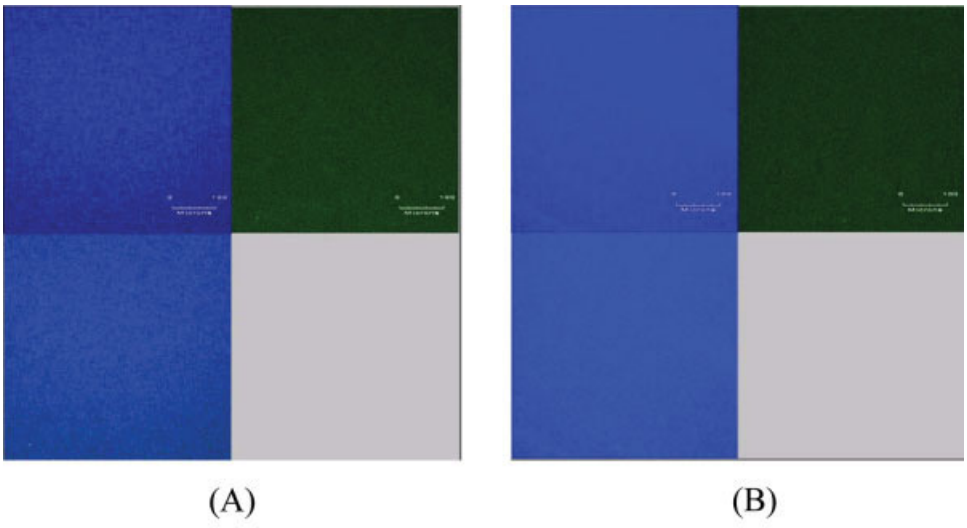

Figure 9 CLSM images of PUD–PWP composite coatings (containing 21.0% PWP) prepared by different mixing techniques: (A) mechanically mixing; (B) micro-homogenization. Upper left box represents protein dye channel (647 nm), upper right box represents autofluorescence (488 nm) of primary binder (PUD), bottom left box represent the merge of both channels (protein dye and autofluorescence), and bottom right represents an extra channel for additional laser line (unused). [Color figure can be viewed in the online issue, which is available at www.interscience.wiley.com.]

TABLE IV
Visual Rating of Mold Growth on the Test Panels According to ASTM D3274–95 Photographic Standards

Samples	Average visual rating
Uncoated panels	6.50 ± 2.66
Simple PUD coated panels[a]	9.67 ± 0.60
PUD–PWP coated panels[b]	8.86 ± 0.90
Simple PUD (+0.3% biocide) coated panels[a]	9.67 ± 0.60
PUD–PWP (+0.3% biocide) coated panels[b]	9.62 ± 0.44
C1 coated panels[c]	8.55 ± 1.01
C2 coated panels[d]	7.93 ± 1.38

[a] Simple PUD, Simple oil-modified polyurethane resin coating.
[b] PUD–PWP, Blended oil-modified polyurethane and polymerized whey protein solution (19.0%) coating.
[c] C1, Commercial water-based polyurethane coating.
[d] C2, Commercial water-based acrylic-polyurethane coating.

correlated with the increased levels of PWP addition. The film structure of the 10.5% PWP sample showed more autofluorescence than films containing higher levels of PWP, indicating that the primary binder component in these films was the oil-modified polyurethane dispersion.

The magnification used in image formation was increased to 60× times 2.5 zoom to obtain a more detailed structural view of the samples (Fig. 8). Figure 8 illustrates the structural differences between the top side (area exposed to air during casting) and the bottom side of the test film (area in contact with Petridish). The intensity of Alexa Fluor® 647 stain was lower in the bottom side of the test film in comparison to that of the top side. This observation indicates that during the drying process, whey proteins that are surface active molecules absorbed more at the air-liquid interface such that a lower concentration of the protein existed at the bottom side of the test film.[24]

To further analyze the method of blending used in this study, the distribution of protein component was examined by comparing two different mixing techniques. Figure 9 illustrates formulations prepared at 21% PWP by mechanically mixing and homogenization (micro-homogenization @ 25,000 RPM). Homogenization resulted in films with increased protein stain intensity and a smoother polymer structure than mechanical mixing of the coating components. This observation suggests that particle coalescence and protein distribution could be further enhanced by using high-speed mixing technique.

Mold growth analysis

The average visual ratings from the mold test analysis are presented in Table IV. Higher levels of mold growth were observed on the surfaces of untreated panels. Panels coated with PUD–PWP dispersion also exhibited higher level of mold growth on the coated surface when compared to panels coated with PUD formulation. However, in comparison to panels coated with commercial products, the PUD–PWP coated panels had lower levels of mold growth on their surfaces.

Repeated measures analysis of variance demonstrated that there was a significant difference ($P < 0.01$) in mold growth between uncoated panels and all treated panels (Table V). No significant difference in mold growth occurred on panels coated with or without biocide addition to simple PUD and PUD–PWP formulations. Commercial water-based polyurethane and acrylic–polyurethane coated panels also showed no significant difference in mold growth compared with panels coated with blended PUD–PWP formulation. However, the addition of biocide to blended PUD–PWP formulation resulted in a significant decrease ($P < 0.05$) in mold growth in comparison to both commercially coated panels.

As early as week 1, a significant increase ($P < 0.05$) in mold growth occurred on uncoated panels in comparison to PUD and blended PUD–PWP treated pan-

TABLE V
Repeated Measures Statistical Analyses between Subject Effects

Treatment comparison	*P*-value
Simple PUD vs. uncoated[a]	<0.0001*
Simple PUD vs. PUD–PWP	0.1181
Simple PUD vs. simple PUD (+0.3% biocide)	1.0000
Simple PUD vs. PUD–PWP (+0.3% biocide)	0.9234
Simple PUD vs. C1	0.0372*
Simple PUD vs. C2	0.0030*
PUD–PWP vs. uncoated[b]	0.0003*
PUD–PWP vs. simple PUD (+0.3% biocide)	0.1181
PUD–PWP vs. PUD–PWP (+0.3% biocide)	0.1394
PUD–PWP vs. C1	0.5346
PUD–PWP vs. C2	0.0768
Simple PUD (+0.3% biocide) vs. uncoated	<0.0001*
Simple PUD (+0.3% biocide) vs. PUD–PWP (+0.3% biocide)	0.9234
Simple PUD (+0.3% biocide) vs. C1	0.0372*
Simple PUD (+0.3% biocide) vs. C2	0.0030*
PUD–PWP (+0.3% biocide) vs. uncoated	<0.0001*
PUD–PWP (+0.3% biocide) vs. C1	0.0448*
PUD–PWP (+0.3% biocide) vs. C2	0.0037*
C1 vs. uncoated[c]	0.0009*
C1 vs. C2	0.2236
C2 vs. uncoated[d]	0.0108*

[a] Simple PUD, Simple oil-modified polyurethane resin coating.
[b] PUD–PWP, Blended oil-modified polyurethane and polymerized whey protein solution (19.0%) coating.
[c] C1, Commercial water-based polyurethane coating.
[d] C2, Commercial water-based acrylic-polyurethane coating.
* Indicates significant differences.

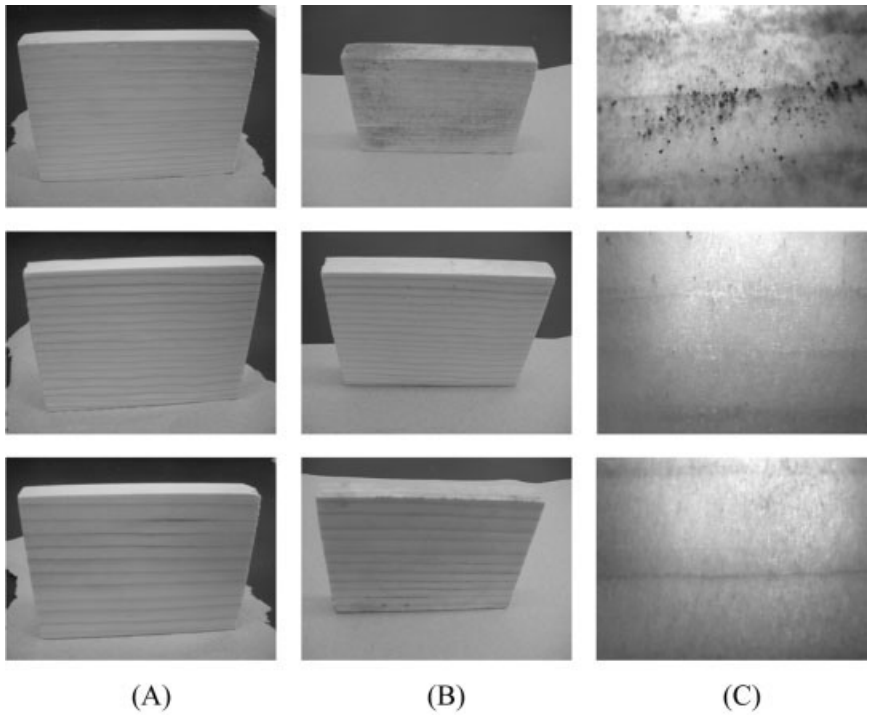

Figure 10 Digital pictures and microstructure images (×10 magnification) of uncoated (top row), simple PUD coated (middle row), and PUD–PWP coated (bottom row) test panels: (A) digital pictures at week 0; (B) digital pictures at week 6; (C) microstructure images obtained at week 6.

els. A significant increase in mold growth on uncoated panels was observed in comparison to water-based polyurethane coated panels after 2 weeks. It was not until week 4 that a significant difference ($P < 0.05$) was observed between uncoated and acrylic–polyurethane coated panels. Significant differences among all other treatments were observed no later than week 3 of the experiment. The level of mold growth on coated panels appeared to increase at a gradual rate over time. The rate of mold growth on uncoated panels showed a rapid increase during the period between week 3 and week 6.

Figures 10 and 11 illustrate digital and microstructure images of mold growth on the test panels at the beginning of the study, week 0, and at the end of the accelerated test, week 6. The appearance and level of mold is apparent in both photographic views. Digital pictures provided an overview of the mold growth on the entire surface of the test panels, while microstructure images provided increased magnification of mold growth at a concentrated area of the test panels. As shown by the microstructure images of the three mold spores used in this study, *A. niger* most heavily colonized on the surface of the test panels. The mold cultures used in this study were chosen because they represent some of the most common species known to cause mold growth on interior coatings.[25] The distribution of mold growth showed no distinguishing patterns on the panels' surfaces. This growth pattern might be due to the environmental conditions of the chamber and also based on the uniformity of applied coatings on the test panels. In Figures 10 and 11, the difference in mold growth between week 0 and week 6 was very obvious on uncoated and acrylic–polyurethane coated digital images. Microstructure images obtained at 10× magnification further illustrated the level of mold growth at week 6 of the experiment.

The growth of mold on coated surfaces is known to be a very slow process and visible evidence can take many years before appearing. The accelerated test used in this study demonstrated significant differences in mold growth on the test panels by week 4 of the experiment. Overall, none of the panels coated with formulations developed in this study received a rating below 8 over a period of 6 weeks. The structural integrity and chemical components of the coatings resulted in limited nutrients available for the growth of mold and fungi, even when PWP was added to the coatings, subjected to very humid conditions.

Although biocide addition resulted in no significant resistance to mold growth between simple PUD and blended PUD–PWP coated panels, a decrease in mold uptake was observed on the test panels when biocide was added. Increasing the level of biocide might further improve the resistance to mold growth. It is recommended that a combination of in-can and dry-film biocide be incorporated into the coating solution to

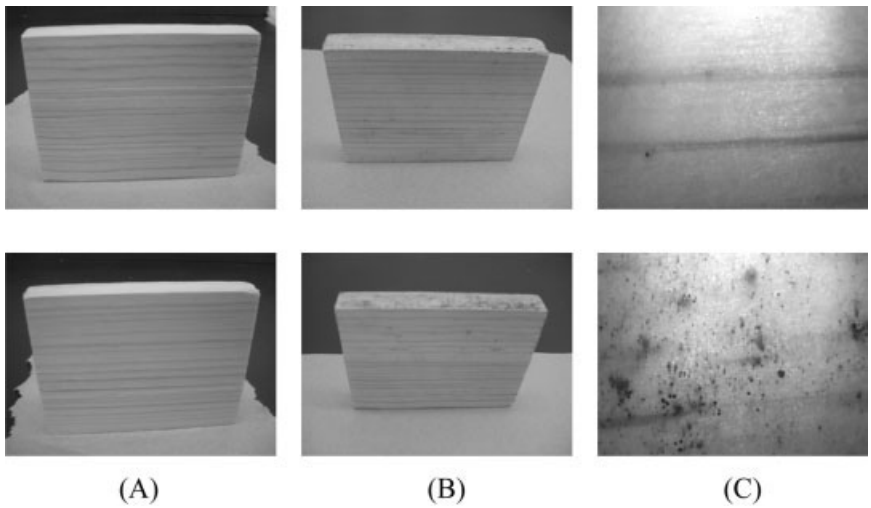

Figure 11 Digital pictures and microstructure images (×10 magnification) of commercial water-based polyurethane coated (top row) and commercial water-based hybrid acrylic–polyurethane coated (bottom row) test panel: (A) digital pictures at week 0; (B) digital pictures at week 6; (C) microstructure images obtained at week 6.

provide the best possible protection against microbial growth.[12]

Increased levels of mold growth observed on commercial acrylic–polyurethane coated panels in comparison to commercial polyurethane coated panels suggests that the lack of particle coalescence, observed in AFM microstructure analysis, is responsible for the poor resistance to mold growth demonstrating the importance of optimized structural cohesiveness.

In addition to using effective broad spectrum biocides, there are different means of reducing the risks of in-can microbial contamination of the product.[11] These include keeping the air inside the factory clean, improving the quality and storage facilities, periodically testing the water used in production, adequately preserving aqueous raw materials to maintain their quality, and adopting good plant hygiene practices.

CONCLUSIONS

The combination of polymerized whey proteins with other binder materials such as oil-modified polyurethane resulted in stable colloidal coating dispersions. AFM and CLSM were effective tools for examination of the polymer coatings. Micrographs of the films obtained demonstrated the blending compatibility between the polymerized whey proteins and the oil-modified polyurethane resins and revealed the details of the interactions among constituents. Application of both techniques provided a broader scope of understanding in regard to microstructural properties of the dry films. The results from the accelerated mold test revealed that mold resistance of the newly developed coatings was not significantly affected by protein addition. Panels coated with the formulation containing a low level of biocide (0.3%) resulted in a significant improvement of resistance to mold growth when compared to panels coated with commercial water-based coatings ($P < 0.05$). The results suggest that a blend of polymerized whey proteins and oil-modified polyurethane may provide the industry with a novel alternative for developing environment-friendly wood-finish products.

References

1. Princen, L. H.; Baker, F. L. Paint Varnish Prod 1971, 61, 21.
2. Provder, T.; Urban, M. W. Film Formation in Coatings: Mechanisms, Properties, and Morphology; American Chemical Society: Washington, DC, 2001.
3. Rynders, R. M.; Hegedus, C. R.; Gilicinski, A. G. J Coat Technol 1995, 67, 59.
4. Serry, F. M.; Strausser, Y. E.; Elings, J.; Magonov, S.; Thornton, J.; Ge, L. In Proceedings of the Twelfth International Conference on Surface Modification Technologies, Rosemont, Illinois, October 12–14, 1998; Surface Modification Technologies XII; Sudarshan, T. S., Khor, K. A., Jeandin, M., Eds.; ASM International: Materials Park, OH, 1998; p 123.
5. Zosel, A. Polym Adv Technol 1995, 6, 263.
6. Kasas, S.; Thomson, N. H.; Smith, B. L.; Hansma, P. K.; Miklossy, J.; Hansma, H. G. Int J Imag Syst Technol 1997, 8, 151.
7. Jandt, K. D. Surf Sci 2001, 491, 303.
8. Gerharz, B.; Kuropka, R.; Petri, H.; Butt, H. J. Prog Org Coat 1997, 32, 75.
9. Paddock, S. W. Biotechniques 1999, 27, 992.
10. Matsumoto, B.; Kramer, T. Cell Vis 1994, 1, 190.
11. Dunk, T. Paintindia 1998, 48, 101.
12. Joshi, C. D. Paintindia 1996, 46, 35.
13. McHugh, T. H.; Aujard, J. F.; Krochta, J. M. J Food Sci 1994, 59, 416.

14. Perez-Gago, M. B.; Krochta, J. M. J Food Sci 2001, 66, 705.
15. Anker, M.; Stading, M.; Hermansson, A. M. J Agric Food Chem 1999, 47, 1878.
16. Li, J.; Guo, M. R. J Dairy Sci 2002, 85(Suppl. 1), 380.
17. Wright, N. C.; Guo, M. R. Abstr Pap Am Chem Soc 2002, 224, 171 (PMSE Part 2).
18. Lent, L.; Vanasupa, L.; Tong, P. J Food Sci 1998, 63, 824.
19. Ming, Y.; Meier, D. J. In Proceedings of the American Chemical Society Division of Polymeric Materials: Science and Engineering, Spring Meeting, San Francisco, California, April 13–17, 1997; American Chemical Society: Washington, DC, 1997; p 25.
20. Jain, N. C. In Proceedings of the Fifteenth International Conference on Surface Modification Technologies, Indianapolis, Indiana, November 5–8, 2001; Surface Modification Technologies XV; Sudarshan, T. S., Stiglich, J. J., Jeandin, M., Eds.; ASM International: Materials Park, OH, 2002; p 87.
21. Hegedus, C. R.; Kloiber, K. A. J Coat Technol 1996, 68, 39.
22. Wu, L.; You, B.; Li, D. J Appl Polym Sci 2002, 84, 1620.
23. Zutara, M. S. Ph.D. Dissertation, University of Vermont, Burlington, Vermont, 2001.
24. Leman, J.; Kinsella, J. E. Crit Rev Food Sci Nutr 1989, 28, 115.
25. Bussjaeger, S.; Daisey, G.; Simmons, R.; Spindel, S.; Williams, S. J Coat Technol 1999, 71, 67.